

Mathematical analysis of the Cancitis model and the role of inflammation in blood cancer progression

Sajid, Zamra; Wienecke Andersen, Morten; Ottesen, Johnny T.

Published in:
Mathematical Biosciences and Engineering

DOI:
[10.3934/mbe.2019418](https://doi.org/10.3934/mbe.2019418)

Publication date:
2019

Document Version
Publisher's PDF, also known as Version of record

Citation for published version (APA):
Sajid, Z., Wienecke Andersen, M., & Ottesen, J. T. (2019). Mathematical analysis of the Cancitis model and the role of inflammation in blood cancer progression. *Mathematical Biosciences and Engineering*, 16(6), 8268-8289. <https://doi.org/10.3934/mbe.2019418>

General rights

Copyright and moral rights for the publications made accessible in the public portal are retained by the authors and/or other copyright owners and it is a condition of accessing publications that users recognise and abide by the legal requirements associated with these rights.

- Users may download and print one copy of any publication from the public portal for the purpose of private study or research.
- You may not further distribute the material or use it for any profit-making activity or commercial gain.
- You may freely distribute the URL identifying the publication in the public portal.

Take down policy

If you believe that this document breaches copyright please contact rucforsk@ruc.dk providing details, and we will remove access to the work immediately and investigate your claim.



Research article

Mathematical analysis of the Cancitis model and the role of inflammation in blood cancer progression

Zamra Sajid, Morten Andersen* and Johnny T. Ottesen

IMFUFA, Department of Science and Environment, Roskilde University, Denmark

* **Correspondence:** Email: moan@ruc.dk; Tel: +4546743936.

Abstract: Recently, a tight coupling has been observed between inflammation and blood cancer such as the Myeloproliferative Neoplasms (MPNs). A mechanism based six-dimensional model - the Cancitis model - describing the progression of blood cancer coupled to the inflammatory system is analyzed. An analytical investigation provides criteria for the existence of physiological steady states, trivial, hematopoietic, malignant and co-existing steady states. The classification of steady states is explicitly done in terms of the inflammatory stimuli. Several parameters are crucial in determining the attracting steady state(s). In particular, increasing inflammatory stimuli may transform a healthy state into a malignant state under certain circumstances. In contrast for the co-existing steady state, increasing inflammatory stimuli may reduce the malignant cell burden. The model provides an overview of the possible dynamics which may inform clinical practice such as whether to use inflammatory inhibitors during treatment.

Keywords: cancer; inflammation; mathematical modelling; steady states; stability

1. Introduction

Myeloproliferative Neoplasms (MPNs) is a group of hematopoietic stem cell disorders, including essential thrombocytosis (ET), polycythemia vera (PV) and primary myelofibrosis (PMF) [1, 2]. The pathogenesis of these neoplasms is yet to be fully discovered. For patients with MPNs, the mutation *JAK2V617F* is found present in the most cases of ET (50%) and in 95% of the cases with PV and PMF ultimately leading to acute myeloid leukemia (AML) [3,4]. This suggests a biological continuum where the diseases evolve from early cancers (ET and PV) into the advanced myelofibrosis stage, with an increasing load of *JAK2V617F* mutations from a low burden at ET and PV to a high load [2, 5]. MPNs imply an increased risk for the development of other cancers [1, 4].

Recent research supports that MPNs can be regarded as chronic inflammatory diseases and MPNs has been described as a "human inflammation model", which leads to premature atherosclerosis, clonal

evolution and an increased risk of second cancers. [2, 3, 6]. This is based on evidence from clinical observations, experiments and molecular studies [3].

Several insightful theoretical studies have been published on control dynamics of biological networks. Mathematical models have been proposed [7–9] describing the control networks for regulation of stem cell lineage. Mathematical modelling of cancer is useful for understanding of cancer initiation, progression [10, 11], to confirm or dismiss biological/medical hypotheses, and to study effects of single or multi modality treatments *in silico*. The mathematical model presented in [12] shows that successful therapy may eliminate tumour stem cells. A five-dimensional model given in [13] includes active and quiescent stem cells, progenitor cells, mature cells and one immune compartment describing chronic myelogenous leukemia. In [14] a mathematical model of cancer stem cell dynamics is proposed and the different scenarios of cancer initiation and possible treatments strategies have been discussed. The mathematical model given in [15] is useful for investigating the impact of cytokine-dependence of acute myeloid leukemic cells. In addition, the model allows distinguishing between cytokine-dependent and cytokine-independent acute myeloid leukemia (AML) and both scenarios are supported by patient data.

However, only a few mathematical models of MPNs exist. Some work includes investigation of the origin of myeloid malignancies with MPNs as a particular example [16]. In [17], a two dimensional model of MPNs is investigated without including the immune response dynamically. The Cancitis model including chronic inflammation as the trigger and driver of MPNs was proposed in [5]. In [5], T-cells are not explicitly considered whereas, in [18], the effect of these cells has been included specifically. The analysis of a two dimensional mathematical model [18] is used to discuss *in silico* effect of existing and novel treatments. The model presented here is identical to the model presented in [5] except for the simpler functional form of the stem cells niche interaction used here and in [18].

In the present paper we conduct a thorough mathematical investigation of the Cancitis model and explore the intricate coupling between inflammation and MPNs. We address the following questions which have not been systematically investigated previously: Which steady states of the system are feasible and which trajectories are attracted to the steady states? How do the number and stability of the steady states change when varying the parameters, in particular, the exogenous inflammatory stimuli, self-renewal and death rates of stem cells, and inhibitory strength of the stem cell niche interaction? Which set of clustered parameters control the dynamics of the system? Does the analysis suggest correlated parameters? The bio-medical applications of the model analysis are discussed, e.g. how the inflammation influences the transition between healthy and diseased states. In addition, the analysis predicts effects of ongoing and potential combination therapies.

2. The Cancitis model

The Cancitis model stated in [5] is illustrated in Figure 1, with the system of differential equations shown in system (2.1). In this section the details of the model and the reasoning behind it is presented.

The model describes the proliferation of hematopoietic stem cells (HSC) into hematopoietic mature cells (HMC) and likewise malignant stem cells (MSC) into malignant mature cells (MMC). Additionally, the model considers the number of dead cells and the level of inflammation. The debris from the dead cells stimulates the immune response, which in turn affects the self-renewal rate of both HSCs and MSCs.

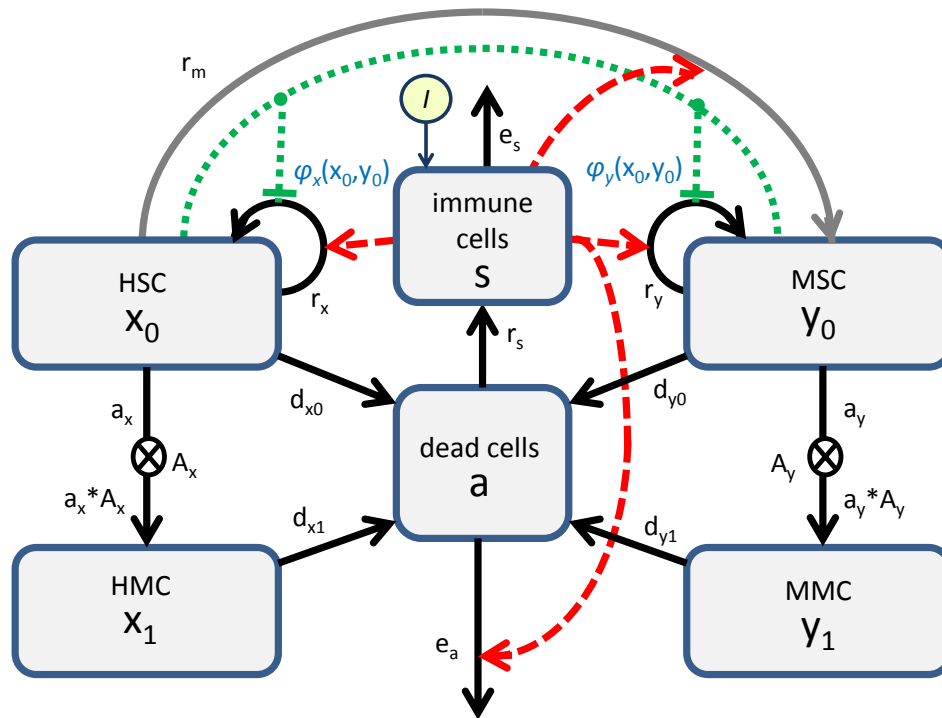


Figure 1. The boxes illustrate the compartments of the Cancitis model. The arrows represent the rates of the flows between and out of these compartments. Red stipulated arrows represent the effect of inflammation which is stimulated by exogenous inflammatory stimuli, I . Green stipulated lines represent the bone marrow niches interaction with a 'crowding' competition between HSC and MSC. Stem cells (HSC and MSC) may self-renew, die or differentiate, while mature cells die after a while (MMC, HMC). Dead cells (a) are engulfed by the immune cells (s), that stimulate production of stem cells, increase risk of mutation and increase the removal of dead cells (For more details, see main text).

The model consists of six ordinary differential equations one for each compartment; the number of HSC (x_0), the number of HMC (x_1), the number of MSC (y_0), the number of MMC (y_1), the number of dead cells (a), and the level of inflammation (s).

The equations are of the general form,

$$\left\{ \begin{array}{l} \text{Change in amount of a} \\ \text{compartment per time} \end{array} \right\} = \left\{ \begin{array}{l} \text{rate of production times} \\ \text{the producing source} \end{array} \right\} - \left\{ \begin{array}{l} \text{rate of elimination times the} \\ \text{amount in the compartment} \end{array} \right\}.$$

and read specifically,

$$\dot{x}_0 = r_x(\phi_x s - \alpha_x)x_0 - r_m s x_0, \quad (2.1a)$$

$$\dot{x}_1 = a_x A_x x_0 - d_{x1} x_1, \quad (2.1b)$$

$$\dot{y}_0 = r_y(\phi_y s - \alpha_y)y_0 + r_m s x_0, \quad (2.1c)$$

$$\dot{y}_1 = a_y A_y y_0 - d_{y1} y_1, \quad (2.1d)$$

$$\dot{a} = d_{x0} x_0 + d_{y0} y_0 + d_{x1} x_1 + d_{y1} y_1 - e_a a s, \quad (2.1e)$$

$$\dot{s} = r_s a - e_s s + I, \quad (2.1f)$$

with

$$\alpha_x = \frac{d_{x0} + a_x}{r_x} \quad \text{and} \quad \alpha_y = \frac{d_{y0} + a_y}{r_y}. \quad (2.2)$$

The expressions for the inhibitory niche feedback are chosen as Michaelis-Menten-like functions in contrast to [5],

$$\phi_x \equiv \phi_x(x_0, y_0) = \frac{1}{1 + c_{xx}x_0 + c_{xy}y_0}, \quad (2.3a)$$

$$\phi_y \equiv \phi_y(x_0, y_0) = \frac{1}{1 + c_{yx}x_0 + c_{yy}y_0}. \quad (2.3b)$$

A stem cell can proliferate in three ways; symmetric self-renewal (resulting in two new stem cells), asymmetric self-renewal (resulting in one stem cell and one progenitor cell) and symmetric differentiation (resulting in two progenitor cells). The rate of self-renewal is denoted as r_x and r_y for HSC and MSC respectively. The self-renewal of stem cells is known to be inhibited by self-regulating niche feedback [19], resulting in decreased self-renewal when the level of stem cells in the bone marrow is high. Adopting the approach taken in [12], [20] and [21], this is implemented by Michaelis-Menten-like functions $\phi_x(x_0, y_0)$ and $\phi_y(x_0, y_0)$, shown in Eq (2.3b). Allowing the feedback to be different for HSC and MSC, the constants c_{xx} and c_{xy} capture the effects of HSC and MSC on the self-renewal of HSC, while c_{yx} and c_{yy} capture the corresponding effects on the self-renewal of MSC. Additionally, the inflammatory level also affects the self-renewal [22, 23]. This leads a to self-renewal term per cell of $r_x \phi_x s$ and $r_y \phi_y s$ for HSC and MSC respectively. The parameter c_{ij} describes the inhibitory strength of the signalling bone marrow niche feedback from cell type j onto cell type i . It is generally assumed that $c_{yy} \leq c_{yx} \leq c_{xy} \leq c_{xx}$, since malignant cells are less sensitive to inhibitive niche feedback than hematopoietic cells [22, 24].

In [25], a multi compartmental model is proposed relying on a single external feedback mechanism. It is shown that the equilibrium level of mature cells depends only on the self-renewal parameters for the HSC and it is independent of the other compartments. Therefore, the progenitor cells are considered as intermediate steps between stem cells and mature cells, and are implicitly accounted for by multiplication factors A_x and A_y for HSC and MSC respectively. The rate at which the HSC reduces in transforming to HMC is denoted by a_x while the similar rate for MSC transforming to MMC is denoted by a_y . As such, the HMC and MMC accordingly increase with rates $a_x A_x$ and $a_y A_y$ respectively. To account for the cell apoptosis, the four types of cells are removed with rates d_{x0} , d_{x1} , d_{y0} and d_{y1} , for the corresponding cell types.

Genetic mutations are by nature to be described as Poisson processes [26–29]. However, not all mutations are malignant; only mutation which happens on a particular location of the DNA, i.e. at specific amino acids causes a specific mutation, e.g. the JAK2V617F mutation. The probability for hitting a specific location is about 1/30000. In [30] the average mutation probability is estimated to 0.0035 per year, which corresponds to a specific mutation probability of $0.0035/30000 = 1.210^{-7}$

per year. Thus, the probability for one specific malignant mutation is about 10^{-7} per cell per year. Moreover, the mutation is affected by the inflammation, s [31, 32], which is explicitly stated, and resulting in the effective mutation rate $r_m s$. Assuming three sequential mutations are needed to generate a specific malignant stem cell the resulting probability becomes much higher (10^{-25} per year per cell if the mutations are assumed independent). This could be implemented in the otherwise deterministic model but it would increase the computational cost, since it depends on both the probability of a single cell mutation and the number of potential mutating cells at a given time, which itself is determined by the preceding mutational history. To avoid such complications we initialize by having a single MSC and none MMC, and put the mutation rate to zero. This is justified by the fact that the probability of a single cell mutating is small compared to the self-renewal of the MSCs. Thus, the first mutation drives the development leaving a later identical mutation insignificant to the dynamics, which is confirmed by numerical simulations.

The number of dead cells has an up-regulatory effect on the immune response denoted r_s . External environmental factors also influence the inflammatory level. This is captured in the model by the term I . Throughout we take $I > 0$, as a perfect sterile environment is an utopic idealization. This term may vary over time due to environmental changes, but in our mathematical analysis we will consider I as piecewise constant. The inflammation, s , is down-regulated naturally by the eliminating rate e_s .

Additionally, the change in the amount of dead cells per time is given by the death rate times the number of cells minus the clearance by the immune system. As given in [33] clearance is described by a second order equation $-e_a a s$ since the engulfed immune cells have to meet the dead cells debris to mediate endocytosis. Thus, clearance is bilinear in both a and s representing the activity of the immune system, eliminating the dead cells with an elimination rate e_a .

Initial conditions for the Cancitis model in equations are needed for the given system of differential equations (2.1–2.3b). Here, we mainly focus on the model after the first mutation, i.e. with $y_0(0) = 1$, $y_1(0) = 0$, $r_m = 0$, and the remaining variables as those in the healthy steady state (see below). All other parameter values are assumed to be positive.

2.1. Steady states of the model

The stable steady states are attractors in the six dimensional phase space. This motivates systematic study of the existence and location of steady states and how this is affected by perturbing parameter values.

Motivated by the biology where the number of cells and concentrations are required to be non-negative numbers, we will use the terminology that a steady state is admissible if and only if all the components are non-negative, i.e. if and only if a steady state is in the non-negative octahedron.

Consider the system of Eqs (2.1–2.3b). For steady state solutions, $\dot{x}_0 = \dot{x}_1 = \dot{y}_0 = \dot{y}_1 = \dot{a} = \dot{s} = 0$,

$$\left(\frac{\bar{s}}{\alpha_x} - (1 + c_{xx}\bar{x}_0 + c_{xy}\bar{y}_0) \right) \bar{x}_0 = 0, \quad (2.4a)$$

$$\left(\frac{\bar{s}}{\alpha_y} - (1 + c_{yx}\bar{x}_0 + c_{yy}\bar{y}_0) \right) \bar{y}_0 = 0, \quad (2.4b)$$

$$\bar{x}_1 = \frac{a_x A_x \bar{x}_0}{d_{x1}}, \quad (2.4c)$$

$$\bar{y}_1 = \frac{a_y A_y \bar{y}_0}{d_{y1}}, \quad (2.4d)$$

$$d_{x0} \bar{x}_1 + d_{x1} \bar{x}_1 + d_{y0} \bar{y}_0 + d_{y1} \bar{y}_1 - e_a \bar{a} \bar{s} = 0, \quad (2.4e)$$

$$\bar{a} = \frac{e_s}{r_s} \left(\bar{s} - \frac{I}{e_s} \right). \quad (2.4f)$$

The values of x_0 , x_1 , y_0 , y_1 , a and s at steady state are denoted as \bar{x}_0 , \bar{x}_1 , \bar{y}_0 , \bar{y}_1 , \bar{a} and \bar{s} respectively. The admissible steady states can be classified as,

- a trivial steady state if and only if $\bar{x}_0 = \bar{y}_0 = 0$,
- a (purely) hematopoietic steady state if and only if $\bar{y}_0 = 0$ and $\bar{x}_0 > 0$,
- a (purely) malignant steady state if and only if $\bar{x}_0 = 0$ and $\bar{y}_0 > 0$, or
- a co-existing steady state if and only if $\bar{x}_0 > 0$ and $\bar{y}_0 > 0$.

The admissibility of steady states necessitates certain inequalities to be fulfilled, which leads to restriction on the parameters, e.g. from Eq (2.4f), non-negativity of \bar{a} requires $\bar{s} \geq \frac{I}{e_s}$. I is assumed to be positive thus $\frac{I}{e_s} > 0$. Hence

$$\bar{s} \geq \frac{I}{e_s} > 0, \quad (2.5)$$

for any admissible steady state. Note that, \bar{x}_1 and \bar{y}_1 are non-negative if and only if \bar{x}_0 and \bar{y}_0 are non-negative, respectively. Substituting expressions of \bar{x}_1 and \bar{y}_1 in Eq (2.4e) gives,

$$e_a \bar{a} \bar{s} = \beta_x \bar{x}_0 + \beta_y \bar{y}_0, \quad (2.6)$$

where $\beta_x = a_x A_x + d_{x0}$ and $\beta_y = a_y A_y + d_{y0}$. Thus, Eqs (2.4e–2.4f) and (2.6) result in a second order equation in \bar{s} having the general solution,

$$\bar{s}_{\pm} = \frac{I}{2e_s} \left(1 \pm \sqrt{1 + \zeta(\beta_x \bar{x}_0 + \beta_y \bar{y}_0)} \right), \quad (2.7)$$

where $\zeta = \frac{4r_s e_s}{e_a I^2} > 0$. \bar{s}_- is negative for positive \bar{x}_0 or \bar{y}_0 . In case, $(\bar{x}_0, \bar{y}_0) = (0, 0)$, Eq (2.7) leads to $\bar{s}_- = 0$ contradicting $\bar{s} > 0$. Thus, $s = \bar{s}_-$ is not biologically realizable and we therefore put $\bar{s} = \bar{s}_+$ in the further analysis. Note that, for non-trivial steady states, $\bar{s} > \frac{I}{e_s}$. In addition, non-negativity of \bar{x}_0 and \bar{y}_0 implies non-negativity of \bar{x}_1 , \bar{y}_1 , \bar{s} and \bar{a} .

Hence, the existence of admissible steady states \bar{x}_0 , \bar{y}_0 , \bar{x}_1 , \bar{y}_1 , \bar{s} and \bar{a} follows from Eqs (2.4a), (2.4b) and (2.7).

Below we make a complete analysis of the existence of various steady states depending on how I relates to the remaining parameters. This choice is due to the fact that the external inflammatory stimuli I is of great interest in health care and to elucidate consequences of using inflammation inhibitors as part of treatment.

Proposition 1. *A trivial steady state E_0 always exists,*

$$E_0 = \left(0, 0, 0, 0, 0, \frac{I}{e_s} \right). \quad (2.8)$$

Proof. Follow directly from Eqs (2.4e) and (2.5). \square

Hematopoietic steady states may exist depending on the rest of the parameter values. As above we chose the inflammatory stimuli I as the leading parameter and make a complete analysis of possible hematopoietic steady states. The analysis of the existence of the hematopoietic steady states depends crucially on the following lumped parameters,

$$I_H = 2\sqrt{\frac{e_s r_s \beta_x}{e_a c_{xx}} - \frac{r_s \beta_x}{e_a c_{xx} \alpha_x}}, \quad (2.9)$$

$$\zeta_{H1} = 2e_s \alpha_x - \frac{r_s \beta_x}{e_a c_{xx} \alpha_x}, \quad (2.10)$$

$$\zeta_{H2} = e_s \alpha_x, \quad (2.11)$$

$$\zeta_{H3} = \frac{r_s \beta_x}{e_s e_a c_{xx}}, \quad (2.12)$$

the last two always being positive.

Proposition 2. *Two hematopoietic steady states $E_{H\pm}$ may exist in the following cases,*

- If $\alpha_x^2 \leq \frac{\zeta_{H3}}{4}$ then E_{H+} exists if and only if $I > 0$.
- If $\frac{\zeta_{H3}}{4} < \alpha_x^2 \leq \zeta_{H3}$ then E_{H+} exists if and only if $I \geq I_H$.
- If $\zeta_{H3} < \alpha_x^2$ then E_{H+} exists if and only if $I > \zeta_{H2}$.
- If $\alpha_x^2 \leq \frac{\zeta_{H3}}{4}$ then E_{H-} exists if and only if $I \leq \zeta_{H2}$.
- If $\frac{\zeta_{H3}}{4} < \alpha_x^2 \leq \zeta_{H3}$ then E_{H-} exists if and only if $I_H \leq I \leq \zeta_{H2}$.
- If $\zeta_{H3} < \alpha_x^2$ then E_{H-} does not exist.

In case of existence, $E_{H+} = (\bar{x}_{0H+}, \bar{x}_{1H+}, 0, 0, \bar{a}_{H+}, \bar{s}_{H+})$ is given by $\bar{x}_{0H+} = \frac{1}{2e_s c_{xx} \alpha_x} (I - \zeta_{H1} + \sqrt{(\zeta_{H1} - I)^2 - 4e_s \alpha_x (\zeta_{H2} - I)})$, $\bar{s}_{H+} = \alpha_x (1 + c_{xx} \bar{x}_{0H+})$, $\bar{a}_{H+} = \frac{\beta_x \bar{x}_{0H+}}{e_a \bar{s}_{H+}}$, and $\bar{x}_{1H+} = \frac{a_x A_x \bar{x}_{0H+}}{d_{x1}}$ whereas $E_{H-} = (\bar{x}_{0H-}, \bar{x}_{1H-}, 0, 0, \bar{a}_{H-}, \bar{s}_{H-})$ is given by $\bar{x}_{0H-} = \frac{1}{2e_s c_{xx} \alpha_x} (I - \zeta_{H1} - \sqrt{(\zeta_{H1} - I)^2 - 4e_s \alpha_x (\zeta_{H2} - I)})$, $\bar{s}_{H-} = \alpha_x (1 + c_{xx} \bar{x}_{0H-})$, $\bar{a}_{H-} = \frac{\beta_x \bar{x}_{0H-}}{e_a \bar{s}_{H-}}$, and $\bar{x}_{1H-} = \frac{a_x A_x \bar{x}_{0H-}}{d_{x1}}$.

Proof. A hematopoietic steady state E_H follows from Eqs (2.4a) and (2.7) with $y_0 = y_1 = 0$ as possible positive solutions to

$$\bar{x}_{0H}^2 + \frac{1}{e_s c_{xx} \alpha_x} (\zeta_{H1} - I) \bar{x}_{0H} + \frac{1}{e_s c_{xx}^2 \alpha_x} (\zeta_{H2} - I) = 0. \quad (2.13)$$

For the solutions to (2.13) to be real,

$$(\zeta_{H1} - I)^2 \geq 4\zeta_{H2}(\zeta_{H2} - I). \quad (2.14)$$

In case $I \geq \zeta_{H2}$, (2.14) is always fulfilled. In case $I < \zeta_{H2}$, (2.14) is equivalent to

$$I^2 + \frac{2r_s \beta_x}{e_a c_{xx} \alpha_x} I + \frac{r_s \beta_x}{e_a c_{xx} \alpha_x} \left(\frac{r_s \beta_x}{e_a c_{xx} \alpha_x} - 4e_s \alpha_x \right) \geq 0. \quad (2.15)$$

Solving for I we get,

$$I \geq I_H = \gamma_x \left(\alpha_x^2 - \frac{\zeta_{H3}}{4} \right), \quad (2.16)$$

with

$$\gamma_x = \frac{\frac{4e_s r_s \beta_x}{e_a c_{xx} \alpha_x^2}}{\frac{r_s \beta_x}{e_a c_{xx} \alpha_x} + 2 \sqrt{\frac{e_s r_s \beta_x}{e_a c_{xx}}}} > 0. \quad (2.17)$$

From Eqs (2.14) and (2.16) it follows that the solutions to Eq (2.13) are real for $I \geq \zeta_{H2}$ or $I_H \leq I < \zeta_{H2}$ in case $I_H < \zeta_{H2}$.

Whenever the solutions to (2.13) are real, they are given by

$$\bar{x}_{0H\pm} := \frac{1}{2e_s c_{xx} \alpha_x} \left(I - \zeta_{H1} \pm \sqrt{(\zeta_{H1} - I)^2 - 4e_s \alpha_x (\zeta_{H2} - I)} \right), \quad (2.18)$$

which depends on the sign of the following five quantities,

$$\zeta_{H1} = 2 \frac{e_s}{\alpha_x} \left(\alpha_x^2 - \frac{\zeta_{H3}}{2} \right), \quad (2.19)$$

$$I_H = \gamma_x \left(\alpha_x^2 - \frac{\zeta_{H3}}{4} \right), \quad (2.20)$$

$$\Delta_{12} = \zeta_{H1} - \zeta_{H2} = \frac{e_s}{\alpha_x} \left(\alpha_x^2 - \zeta_{H3} \right), \quad (2.21)$$

$$\Delta_{H1} = \zeta_{H1} - I_H = \frac{e_s}{\alpha_x + \sqrt{\zeta_{H3}}} \left(\alpha_x^2 - \zeta_{H3} \right), \quad \text{and} \quad (2.22)$$

$$\Delta_{H2} = I_H - \zeta_{H2} = -\frac{e_s}{\alpha_x (\alpha_x + \sqrt{\zeta_{H3}})^2} \left(\alpha_x^2 - \zeta_{H3} \right)^2 \leq 0, \quad (2.23)$$

where the last one immediately implies that the criteria for real solutions of Eq (2.13) is $I \geq I_H$. If the solutions, $\bar{x}_{0H\pm}$, are positive and real, then the formulas for the remaining variables easily follow from Eqs (2.4a–2.4f).

To continue we first consider \bar{x}_{0H+} and afterwards \bar{x}_{0H-} .

For $\alpha_x^2 \leq \frac{\zeta_{H3}}{4}$, it follows from Eqs (2.19)–(2.22) that $\zeta_{H1} < 0$, $\zeta_{H1} < \zeta_{H2}$, $I_H \leq 0$, and $\zeta_{H1} < I_H$. Thus, $\bar{x}_{0H+} > 0$ if and only if $I > 0$.

For $\frac{\zeta_{H3}}{4} < \alpha_x^2 \leq \frac{\zeta_{H3}}{2}$, it follows from Eqs (2.19)–(2.22) that $\zeta_{H1} \leq 0$, $\zeta_{H1} < \zeta_{H2}$, $I_H > 0$, and $\zeta_{H1} < I_H$. Thus, $\bar{x}_{0H+} > 0$ if and only if $I > I_H$.

For $\frac{\zeta_{H3}}{2} < \alpha_x^2 \leq \zeta_{H3}$, it follows from Eqs (2.19)–(2.22) that $\zeta_{H1} > 0$, $\zeta_{H1} \leq \zeta_{H2}$, $I_H > 0$, $\zeta_{H1} < I_H$, and $I_H \leq \zeta_{H2}$. Thus, $\bar{x}_{0H+} > 0$ if and only if $I > I_H$.

For $\zeta_{H3} < \alpha_x^2$ are $\zeta_{H1} > 0$, it follows from Eqs (2.19)–(2.23) that $\zeta_{H1} > \zeta_{H2}$, $I_H > 0$, $\zeta_{H1} > I_H$, and $I_H \leq \zeta_{H2}$. Thus, $\bar{x}_{0H+} > 0$ if and only if $I > \zeta_{H2}$.

Similar, \bar{x}_{0H-} is real if and only if $I \geq I_H$ and $\zeta_{H1} < I < \zeta_{H2}$.

For $\alpha_x^2 \leq \frac{\zeta_{H3}}{4}$, it follows from Eqs (2.19) and (2.20) that $\zeta_{H1} < 0 < \zeta_{H2}$, and $I_H \leq 0$. Thus, $\bar{x}_{0H-} > 0$ if and only if $I < \zeta_{H2}$.

For $\frac{\zeta_{H3}}{4} < \alpha_x^2 \leq \frac{\zeta_{H3}}{2}$, it follows from Eqs (2.19), (2.20) and (2.23) that $\zeta_{H1} \leq 0 < \zeta_{H2}$, $I_H > 0$, and $I_H < \zeta_{H2}$. Thus, $\bar{x}_{0H-} > 0$ if and only if $I_H \leq I < \zeta_{H2}$.

For $\frac{\zeta_{H3}}{2} < \alpha_x^2 \leq \zeta_{H3}$, it follows from Eqs (2.19)–(2.21) and (2.23) that $0 < \zeta_{H1} < \zeta_{H2}$, $I_H > 0$, and

$I_H < \zeta_{H2}$. Thus, $\bar{x}_{0H-} > 0$ if and only if $I_H \leq I < \zeta_{H2}$.

For $\zeta_{H3} < \alpha_x^2$, it follows from Eqs (2.20) and (2.21) that $\zeta_{H1} > \zeta_{H2}$ and $I_H > 0$. Thus, $\bar{x}_{0H-} > 0$ if and only if $\zeta_{H1} < I < \zeta_{H2}$, which is a contradiction. \square

The conditions for the existence of the **hematopoietic steady states** are summarized in Table 1.

Table 1. Summarizing necessary and sufficient criteria for admissibility of E_H . The first column conditions how α_x is related to ζ_{H3} , the middle column shows the existence conditions for E_{H+} and the last column shows the existence conditions for $E_{H\pm}$ explicitly in terms of I .

For	Only E_{H+} if	Both E_{H+} and E_{H-} if
$\alpha_x^2 < \frac{\zeta_{H3}}{4}$	$I > \zeta_{H2}$	$I \leq \zeta_{H2}$
$\frac{\zeta_{H3}}{4} < \alpha_x^2 < \zeta_{H3}$	$I > \zeta_{H2}$	$I_H \leq I \leq \zeta_{H2}$
$\zeta_{H3} < \alpha_x^2$	$I > \zeta_{H2}$	\emptyset

Malignant steady states may exist depending on the range of the parameters. As above we chose the inflammatory stimuli I as our leading parameter and make a complete analysis of possible malignant steady states. The analysis of the existence of the malignant steady states depends crucially on the following lumped parameters,

$$I_H = 2\sqrt{\frac{e_s r_s \beta_y}{e_a c_{yy}}} - \frac{r_s \beta_y}{e_a c_{yy} \alpha_y}, \quad (2.24)$$

$$\zeta_{L1} = 2e_s \alpha_y - \frac{r_s \beta_y}{e_a c_{yy} \alpha_y}, \quad (2.25)$$

$$\zeta_{L2} = e_s \alpha_y, \quad (2.26)$$

$$\zeta_{L3} = \frac{r_s \beta_y}{e_s e_a c_{yy}}, \quad (2.27)$$

the last two being positive.

Proposition 3. *Two malignant steady states $E_{L\pm}$ may exist in the following cases,*

- If $\alpha_y^2 \leq \frac{\zeta_{L3}}{4}$ then E_{L+} exists if and only if $I > 0$.
- If $\frac{\zeta_{L3}}{4} < \alpha_y^2 \leq \zeta_{L3}$ then E_{L+} exists if and only if $I \geq I_L$.
- If $\zeta_{L3} < \alpha_y^2$ then E_{L+} exists if and only if $I > \zeta_{L2}$.
- If $\alpha_y^2 \leq \frac{\zeta_{L3}}{4}$ then E_{L-} exists if and only if $I \leq \zeta_{L2}$.
- If $\frac{\zeta_{L3}}{4} < \alpha_y^2 \leq \zeta_{L3}$ then E_{L-} exists if and only if $I_L \leq I \leq \zeta_{L2}$.
- If $\zeta_{L3} < \alpha_y^2$ then E_{L-} does not exist.

In case of existence, $E_{L+} = (0, 0, \bar{y}_{0L+}, \bar{y}_{1L+}, \bar{a}_{L+}, \bar{s}_{L+})$ is given by $\bar{y}_{0L+} = \frac{1}{2e_s c_{yy} \alpha_y} (I - \zeta_{L1} + \sqrt{(\zeta_{L1} - I)^2 - 4e_s \alpha_y (\zeta_{L2} - I)})$, $\bar{s}_{L+} = \alpha_y (1 + c_{yy} \bar{y}_{0L+})$, $\bar{a}_{L+} = \frac{\beta_y \bar{y}_{0L+}}{e_a \bar{s}_{L+}}$,

and $\bar{y}_{1L+} = \frac{a_x A_x \bar{y}_{0L+}}{d_{y1}}$ whereas $E_{L-} = (0, 0, \bar{y}_{0L-}, \bar{y}_{0L-}, \bar{a}_{L-}, \bar{s}_{L-})$ is given by $\bar{y}_{0L-} = \frac{1}{2e_s c_{yy} \alpha_y} \left(I - \zeta_{L1} - \sqrt{(\zeta_{L1} - I)^2 - 4e_s \alpha_y (\zeta_{L2} - I)} \right)$, $\bar{s}_{L-} = \alpha_y (1 + c_{yy} \bar{y}_{0L-})$, $\bar{a}_{L-} = \frac{\beta_y \bar{y}_{0L-}}{e_a \bar{s}_{L-}}$, and $\bar{y}_{1L-} = \frac{a_x A_x \bar{y}_{0L-}}{d_{y1}}$.

Proof. Due to symmetry in indices x and y , the proof for the malignant case is equivalent to that for the hematopoietic case except index H has to be substituted by L . \square

The result is summarized in Table 2.

Table 2. Summarizing necessary and sufficient criteria for admissibility of E_L . The first column conditions how α_y is related to ζ_{L3} , the middle column shows the existence conditions for E_{L+} and the last column shows the existence conditions for $E_{L\pm}$ explicitly formulated in terms of I .

For	Only E_{L+} if	Both E_{L+} and E_{L-} if
$\alpha_y^2 < \frac{\zeta_{L3}}{4}$	$I > \zeta_{L2}$	$I \leq \zeta_{L2}$
$\frac{\zeta_{L3}}{4} < \alpha_y^2 < \zeta_{L3}$	$I > \zeta_{L2}$	$I_L \leq I \leq \zeta_{L2}$
$\zeta_{L3} < \alpha_y^2$	$I > \zeta_{L2}$	\emptyset

The existence of a **co-existing steady state**

$$E_C = (\bar{x}_{0C}, \bar{x}_{1C}, \bar{y}_{0C}, \bar{y}_{1C}, \bar{a}_C, \bar{s}_C),$$

is far more cumbersome to deal with, since a wealth of sub-cases may arrive depending on various inequality-relations between the parameters. To avoid many tedious but straight forward calculations we limit ourself to the non-degenerate cases where $\zeta_{C1} = \alpha_y c_{yx} - \alpha_x c_{xx} \neq 0$ and $\zeta_{C2} = \alpha_y c_{yy} - \alpha_x c_{xy} \neq 0$.

From Eqs (2.4a and 2.4b), a linear relation between \bar{x}_0 and \bar{y}_0 directly follows,

$$\zeta_{C1} \bar{x}_{0C} + \zeta_{C2} \bar{y}_{0C} - \zeta_{C3} = 0, \quad (2.28)$$

where $\zeta_{C3} = \alpha_x - \alpha_y$. Thus, for the non-degenerate cases,

$$\bar{y}_{0C} = \frac{\zeta_{C1}}{\zeta_{C2}} \left(\frac{\zeta_{C3}}{\zeta_{C1}} - \bar{x}_{0C} \right), \quad (2.29)$$

which geometrically corresponds to a straight line through $(0, \frac{\zeta_{C3}}{\zeta_{C2}})$ and $(\frac{\zeta_{C3}}{\zeta_{C1}}, 0)$. Hence, two generic cases arrive, for $(0, \frac{\zeta_{C1}}{\zeta_{C2}})$ corresponding to positive slope, $\frac{\zeta_{C1}}{\zeta_{C2}} < 0$ corresponding to negative slope, $\frac{\zeta_{C1}}{\zeta_{C2}} > 0$. The first case defines a half line in the positive octahedron and in this case $\bar{x}_{0C} \in (\max\{0, \frac{\zeta_{C3}}{\zeta_{C1}}\}; \infty)$ and $\bar{y}_{0C} \in (\max\{0, \frac{\zeta_{C3}}{\zeta_{C2}}\}; \infty)$. The second case corresponds to either no admissible solution (if and only if $\frac{\zeta_{C3}}{\zeta_{C2}} < 0$ and $\frac{\zeta_{C3}}{\zeta_{C1}} < 0$) or a line segment in the positive octahedron which requires that $\frac{\zeta_{C3}}{\zeta_{C2}} > 0$ and $\frac{\zeta_{C3}}{\zeta_{C1}} > 0$ and in that case are $\bar{x}_{0C} \in (0, \frac{\zeta_{C3}}{\zeta_{C1}})$ and $\bar{y}_{0C} \in (0, \frac{\zeta_{C3}}{\zeta_{C2}})$. From Eq (2.4a) and (2.29),

$$\bar{s}_C = m_1 \bar{x}_{0C} + m_0, \quad (2.30)$$

with $m_0 = \alpha_x(c_{xy}\frac{\zeta_{C3}}{\zeta_{C2}} + 1)$ and $m_1 = \alpha_x(c_{xx} - c_{xy}\frac{\zeta_{C1}}{\zeta_{C2}})$. Before continuing, it is emphasized that $\zeta_1, \zeta_2, \zeta_3, m_0,$ and m_1 all are independent of I but may be positive, negative or in case of m_0 and m_1 zero. From Eq (2.7) it follows that a real and positive \bar{s} exist for $(\bar{x}_{0C}, \bar{y}_{0C}) \in \mathbb{R}_+ \times \mathbb{R}_+$,

$$\bar{s}_C = \frac{I}{2e_s} \left(1 + \sqrt{1 + \frac{\zeta_0}{I^2}(\beta_x \bar{x}_{0C} + \beta_y \bar{y}_{0C})} \right) \quad (2.31)$$

where $\zeta_0 = \frac{4r_s e_s}{e_a} > 0$. Similarly, a negative real root exists. Substituting (2.29) into (2.31) give,

$$\bar{s}_C = \frac{I}{2e_s} + \sqrt{\left(\frac{I}{2e_s}\right)^2 + \frac{\zeta_0 \beta_y \zeta_{C3}}{4e_s^2 \zeta_{C2}} + \frac{\zeta_0}{4e_s^2} \left(\beta_x - \beta_y \frac{\zeta_{C3}}{\zeta_{C2}}\right) \bar{x}_{0C}}. \quad (2.32)$$

Combining Eq (2.30) and (2.32) results in,

$$n_0 - I + n_1 \bar{x}_{0C} = \sqrt{I^2 + n_2 + n_3 \bar{x}_{0C}}, \quad (2.33)$$

where $n_0 = 2e_s m_0, n_1 = 2e_s m_1, n_2 = \frac{\zeta_0 \beta_y \zeta_{C3}}{\zeta_{C2}}$ and $n_3 = \zeta_0 \left(\beta_x - \beta_y \frac{\zeta_{C1}}{\zeta_{C2}}\right)$.

Note that Eq (2.33) has no real solution if either of $f(x) = n_0 - I + n_1 x$ and $g(x) = I^2 + n_2 + n_3 x$ are negative. Thus, if both $f(x)$ and $g(x)$ are positive, Eq (2.33) is equivalent to,

$$n_1^2 x^2 + (2n_1(n_0 - I) - n_3)x + (n_0^2 - n_2 - 2n_0 I) = 0, \quad (2.34)$$

which may have up to two real positive solutions. Hence, there can be at most two coexistence steady states. More specifically,

$$x_{0C+} = -\frac{2n_1(n_0 - I) - n_3}{2n_1^2} + \sqrt{\left(\frac{2n_1(n_0 - I) - n_3}{2n_1^2}\right)^2 - \frac{n_0^2 - n_2 - 2n_0 I}{n_1}}, \quad (2.35)$$

is positive if and only if $f(x_{0C+}) > 0, g(x_{0C+}) > 0,$ and

$$\frac{n_0^2 - n_2 - 2n_0 I}{n_1} < 0 \quad \text{or} \quad \frac{2n_1(n_0 - I) - n_3}{n_1^2} < 0. \quad (2.36)$$

Similar,

$$x_{0C-} = -\frac{2n_1(n_0 - I) - n_3}{2n_1^2} - \sqrt{\left(\frac{2n_1(n_0 - I) - n_3}{2n_1^2}\right)^2 - \frac{n_0^2 - n_2 - 2n_0 I}{n_1}}, \quad (2.37)$$

is positive if and only if $f(x_{0C-}) > 0, g(x_{0C-}) > 0,$ and

$$\frac{2n_1(n_0 - I) - n_3}{2n_1^2} > \frac{n_0^2 - n_2 - 2n_0 I}{n_1} > 0 \quad \text{and} \quad \frac{2n_1(n_0 - I) - n_3}{2n_1^2} < 0. \quad (2.38)$$

Note, some possibilities of equality signs in the inequalities are left out for simplification reasons. Equality may occur on a set of measure zero which is unlikely for a noisy biological system and including these possibilities makes the analysis much more messy. For practical purposes one may first calculate the two (possibly complex) roots x of Eq (2.34) and afterwards examine whether these are real and positive, whether $f(x) > 0$ and $g(x) > 0,$ and whether the corresponding \bar{y}_{0C} calculated from Eq (2.29) is positive, thus the remaining component of E_C will be positive too and the steady state admissible.

Continuing analytically is possible but becomes somehow cumbersome and instead we point out that for any choice of parameter values, there can be at most two coexistence steady states, their existence and value depending on the admissibility of x_{0C+} (Eq (2.35)) and x_{0C-} (Eq (2.37)).

3. Stability and bifurcation analysis

In this section we analytically and numerically examine the stability properties of the various admissible steady states of Eq (2.1) in terms of selected parameters.

3.1. Stability properties of the trivial steady state

The Jacobian of the trivial steady states E_0 is a triangular matrix and four of the six eigenvalues, $-d_{x1}$, $-d_{y1}$, $-e_s$ and $\frac{-Ie_a}{e_s}$, are negative but the two, $\frac{r_x}{e_s}(I - e_s\alpha_x)$ and $\frac{r_y}{e_s}(I - e_s\alpha_y)$, may be positive, negative, zero. Thus, by the Hartman-Grobman Theorem [34]

Lemma 1. E_0 is asymptotically stable if $I < e_s \min\{\alpha_x, \alpha_y\}$, whereas it is unstable if $I > e_s \min\{\alpha_x, \alpha_y\}$.

At $E_{H\pm}$ the Jacobian for the hematopoietic states can be calculated (see Supplementary) and the resulting sixth order characteristic equation shows that $E_{H\pm}$ are stable for

$$\bar{s}_H < \alpha_y(1 + c_{yx}\bar{x}_{0H}). \quad (3.1)$$

However, this is not the generic case, since $\alpha_y < \alpha_x$ (and $c_{yx} \leq c_{xx}$), which contradicts $\bar{s}_H = \alpha_x(1 + c_{xx}\bar{x}_{0H})$. Intensive numerical investigations shows that $E_{H\pm}$ are unstable.

The stability of E_L is similar to that for the hematopoietic steady state except that it is stable if

$$\bar{s}_L < \alpha_x(1 + c_{xy}\bar{y}_{0L}), \quad (3.2)$$

which is fulfilled in the generic case, since $\alpha_x < \alpha_y$ (and $c_{xy} \leq c_{yy}$). This follows from $\bar{s}_L = \alpha_y(1 + c_{yy}\bar{y}_{0L})$. The Jacobian may be found in supplementary.

Lastly, consider the **co-existing steady state**. The Jacobian at E_C may be found in supplementary. However, it is hard to prove any result analytically and we therefore do the stability investigation numerically the in next section.

3.1.1. Numerical Simulations and treatment scenarios

In this section, we focus on numerical results. The default values of parameters used in Figure 2 are given in Table 3. The values are the same as given in [18].

Table 3. Default parameter values and their lumped counterpart.

Parameter	Value	Unit	Parameter	Value	Unit
r_x	$8.7 \cdot 10^{-4}$	day ⁻¹	r_y	$1.3 \cdot 10^{-3}$	day ⁻¹
a_x	$1.1 \cdot 10^{-5}$	day ⁻¹	a_y	$1.1 \cdot 10^{-5}$	day ⁻¹
A_x	$4.7 \cdot 10^{13}$	-	A_y	$4.7 \cdot 10^{13}$	-
d_{x_0}	$2 \cdot 10^{-3}$	day ⁻¹	d_{y_0}	$2 \cdot 10^{-3}$	day ⁻¹
d_{x_1}	129	day ⁻¹	d_{y_1}	129	day ⁻¹
c_{xx}	$5.6 \cdot 10^{-5}$	-	c_{yx}	$5.2 \cdot 10^{-5}$	-
c_{xy}	$5.4 \cdot 10^{-5}$	-	c_{yy}	$5.0 \cdot 10^{-5}$	-
e_s	2	day ⁻¹	r_s	$3 \cdot 10^{-4}$	day ⁻¹
e_a	$2 \cdot 10^9$	day ⁻¹	I	7	day
α_x	2.31	-	α_y	1.54	-
β_x	$5.17 \cdot 10^8$	-	β_y	$5.17 \cdot 10^8$	-
ζ_0	$1.2 \cdot 10^{-12}$	-	ζ_{C1}	$-4.9 \cdot 10^{-5}$	-
ζ_{C2}	$7.4146 \cdot 10^{-4}$	-	ζ_{C3}	0.7646	-
n_0	9.76	-	n_1	-0.51	-
n_2	0.64	-	n_3	$6.61 \cdot 10^{-4}$	-
ζ_{H1}	8.65	-	ζ_{H2}	4.62	-
ζ_{L1}	5.18	-	ζ_{L2}	3.09	-
ζ_{H3}	0.69	-	ζ_{L3}	0.7646	-

The model has been investigated for various choices of parameter values. In Figure 2, clusters of five important parameters, $C = \frac{c_{xx}}{c_{yy}}$, $\mathcal{R} = \frac{\zeta_{H2}}{\zeta_{L2}} = \frac{\alpha_x}{\alpha_y}$ and I are considered to investigate the number of steady states and their stability. In the default case $\mathcal{R} > 1$ (Figure 2a), a trivial steady state always exists, and for low inflammation, i.e., $I < \zeta_{L2}$ it is stable otherwise it is unstable. For $I > \zeta_{L2}$, a purely malignant steady state becomes admissible. For values of I where the trivial and the malignant steady states are admissible, the malignant steady state is stable whereas the trivial steady state is unstable. An unstable hematopoietic steady state becomes admissible as I becomes larger than the threshold value ζ_{H2} , and increasing I further causes emergence of a stable co-existing steady state while the malignant steady state becomes unstable. Thus, for $I > \zeta_{H2}$ and C sufficiently small, four steady states appear namely the trivial, the hematopoietic, the malignant and the co-existing steady states where the co-existing steady state is stable and the rest are unstable. This illustrates that the co-existing steady state depends on I , C and \mathcal{R} . Increasing C from a small, initial value makes the co-existing steady state vanish and the malignant steady state becomes stable whereas the trivial and the hematopoietic steady states remain unstable.

Secondly, consider the second case where $\mathcal{R} = 1$ implying that $\zeta_{H2} = \zeta_{L2}$ (Figure 2b). Increasing I across this value generates an unstable hematopoietic steady state and a malignant steady state simultaneously. For $C < 1$ the malignant steady state is unstable, and a stable coexistence steady state is created as I increase past ζ_{H2} . For $C > 1$ no coexistence steady state is created, instead the malignant steady state is stable. Hence, for $\mathcal{R} = 1$, decreasing C may change the topology from a stable malignant steady state to a stable coexistence steady state i.e. improving the prognosis from disease escape to disease equilibrium. The stable co-existing steady state bifurcates from the trivial steady state and re-

mains stable until $C = 1$. As C exceeds 1, the co-existing steady state disappears, the malignant steady state becomes stable and the trivial and the hematopoietic steady state become unstable.

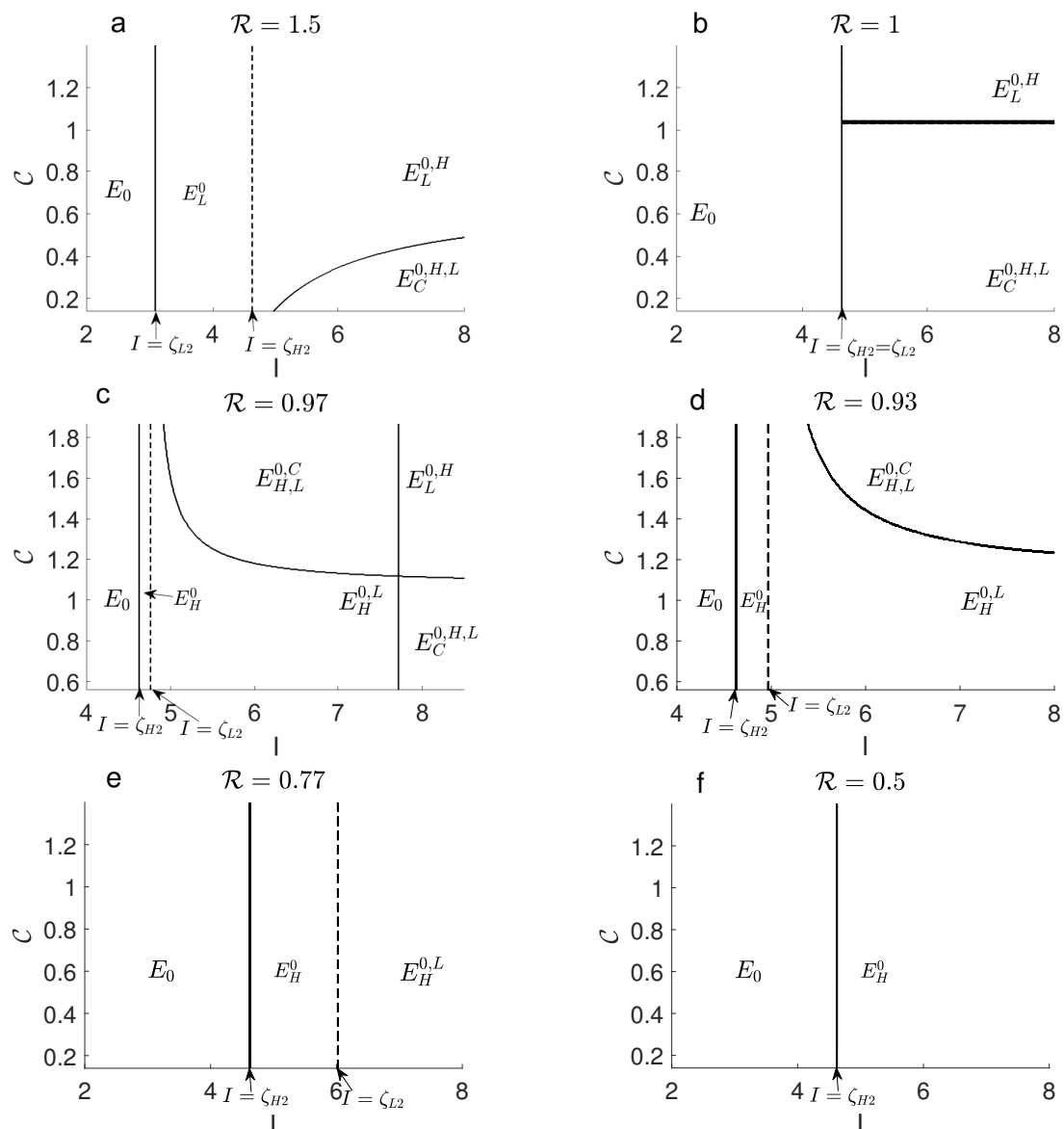


Figure 2. Admissibility and stability of the steady states depending on the parameters I and C for different values of \mathcal{R} . Crossing a solid curve implies a change in which type of stable steady state exists i.e. trivial, malignant, hematopoietic or coexistence. Crossing a dotted curves implies the same steady state is stable in both regions but the number of steady states is changed. The stable steady states are written as subscript of E and unstable steady states are written as superscript of E .

In the remaining panels, $\mathcal{R} < 1$, which implies that a stable hematopoietic steady state is created as the first transition to appear when increasing I from low values past the threshold value ζ_{H2} . Simultaneously, the trivial steady state becomes unstable. In Figure 2c where $\mathcal{R} = 0.97$ the hematopoietic steady

state remains stable for low values of C until I passes a threshold value where a stable coexistence steady state is created leaving the hematopoietic steady state unstable.

For larger values of C there is no coexistence steady state. Instead, as I is increased, a region of bistability appears with a stable hematopoietic steady state and a stable malignant steady state. Increasing I further the hematopoietic steady state becomes unstable. Hence, to reduce disease load, in the case of $\mathcal{R} < 1$, and large values of C and I , it may be optimal treatment to reduce the C value prior to reducing the inflammatory level to avoid being stuck in the basin of attraction of the malignant steady state.

In Figure 2d where $\mathcal{R} = 0.93$, the coexistence steady state no longer appears, the region of bistability has shrunk and a hematopoietic stable steady state is more dominant.

In Figure 2e and f, \mathcal{R} is decreased to 0.77 and 0.5 respectively, and the bistability region is no longer visible. For $I > \zeta_{H2}$ a hematopoietic steady state is the only stable steady state. Figure 2 indicates that reducing C and \mathcal{R} should be targets of intervention. A reduction of I may improve prognosis as well, for example for parameter values as in 2c.

4. Discussion and conclusion

A mechanism-based model published in [5] - the Cancitis model - describing the interaction of the hematopoietic cells, malignant cells and inflammation is analysed here. A thorough mathematical investigation of the model is presented in this paper which did not appear previously. We conducted an analytical analysis of the steady states and showed that four kinds of steady states may exist i.e. trivial, hematopoietic, malignant and co-existing steady states. We characterized the stability of each of these steady states and identified transitions conditions in the number of steady states and in their stability. Trivial, hematopoietic, malignant and coexistence steady states all appear for some parameter values. The steady states are highly relevant as all trajectories appear to approach a steady state after some time - see Figure 3. The case of bistability is visualized in the bottom right panel of Figure 3, with the basin of attraction shown in the (x_0, y_0) -plane using initial condition $(x_1, y_1, a, s) = (4 \times 10^{11}, 4 \times 10^{11}, 600, 2)$. The initial conditions for x_0 and y_0 are varied in a range $1 - 10^5$. The malignant steady state has a large basin of attraction (region (i)), while region (ii) marks the basin of attraction for the hematopoietic steady state.

The intuitive interpretation in most bio-medical literature attributes the main cause for cancer development to the frequency of stem cell division. Another main cause is the regulatory feedback that allows stem cells residing in niche to further divide into blood cell required in blood stream. Our investigation is in agreement with this perception and quantifies this intuitive concept. Furthermore, it shows that stem cell population is important to target in treatment to prevent disease progression.

In [14] and [15] a model without immune interaction is presented. The authors discuss a fraction similar to \mathcal{R} and show that it is important for the dynamics of the system. It has been shown [15] that the leukemic cell load can be temporarily reduced if the growth of HSC is larger than that of leukemic cells for cytokine-dependent AML.

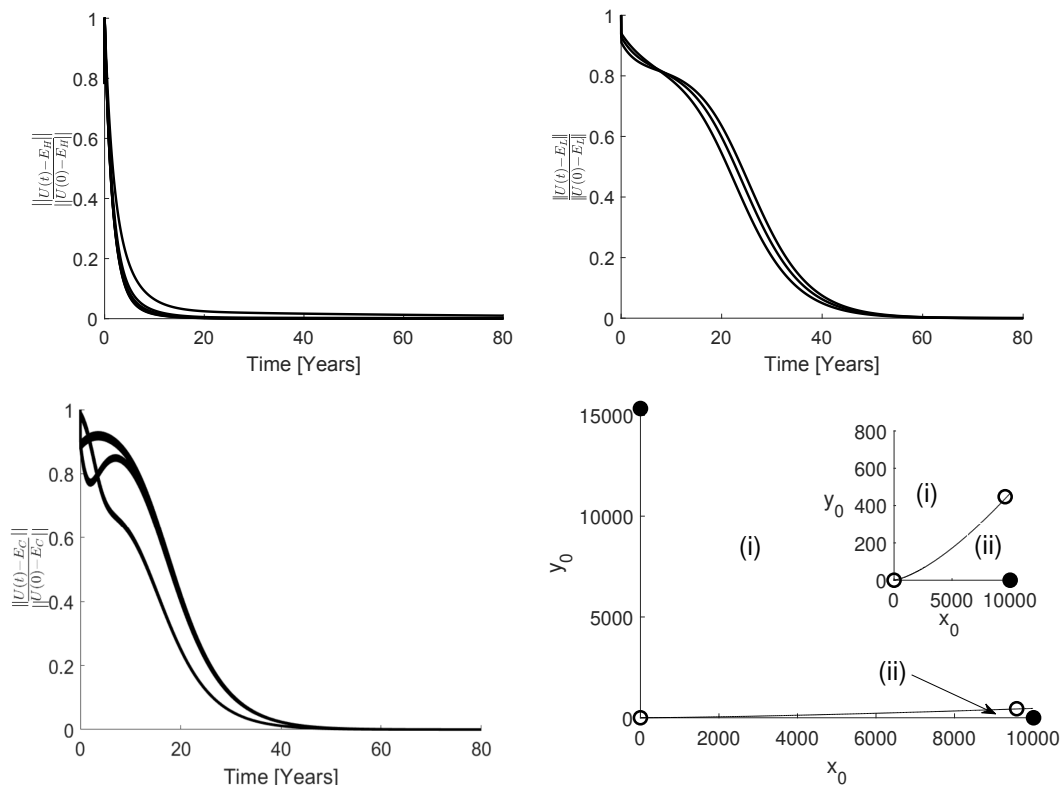


Figure 3. The first three panels illustrate that when a unique, stable steady state exists, it is globally attracting (based on a numerical argument). $U(t)$ denotes the solution of the six-dimensional model 2.1. In the top left panel, $\frac{\|U(t)-E_H\|}{\|U(0)-E_H\|}$ is plotted against time for three different initial conditions. It corresponds to the region where E_H is stable with $C = 0.8$, $\mathcal{R} = 0.97$ and $I = 6$. $\frac{\|U(t)-E_H\|}{\|U(0)-E_H\|}$ tending to zero for large time implies that $U(t)$ is close to E_H for large time. The top right panel shows the stability of E_L with $C = 0.2$, $\mathcal{R} = 1.5$ and $I = 4$. The bottom left panel shows the stability of E_C with $C = 0.1$, $\mathcal{R} = 1.5$ and $I = 7$. The bottom right panel corresponds to bi-stability of E_H and E_L with $C = 1.4$, $\mathcal{R} = 0.97$. The solution to the 6D model is projected onto the x_0 and y_0 plane. Region (i) denotes the set of initial conditions with trajectories converging to E_L whereas region (ii) denotes that trajectories converge to E_H . Black circles show four steady states, E_0 , E_H , E_L and E_C , where filled circle shows stable steady states and empty circle shows unstable steady states.

It is generally assumed that $c_{yy} \leq c_{xx}$ since malignant cells might be less sensitive to environmental crowding [22] and [24]. The ratio C of inhibition of the hematopoietic relative to malignant cells is one of several important prognostic markers. For large values of I , bi-stable and mono-stable regions depend upon C . It can be observed in Figure 2 that for small values of C , i.e., $c_{yy} \geq c_{xx}$, either the hematopoietic steady state is stable or the co-existing steady state is stable which can be interpreted as a good prognosis. However, large values of C may lead to a worse situation, e.g. in one case, the malignant steady state is stable or there exists bi-stability of the hematopoietic and the malignant steady states (see Figure 2c). In addition to the ratio of inhibitive niche feedback, the ratio \mathcal{R} is also important to consider, since it determines how robust the hematopoietic condition may be and how disastrously a

potential blood cancer disease will develop. Thus for $\mathcal{R} > 1$ we have a more serious situation than for $\mathcal{R} < 1$ showing that if this reproduction ratio exceeds the threshold $\mathcal{R}_0 = 1$, it is more disastrous than if it is below \mathcal{R}_0 .

The *JAK2V617F* allele burden is expected to increase due to the expansion of malignant cells. The *JAK2V617F* allele burden is interpreted as the ratio of malignant cells to the total number of mature cells. The model predicted *JAK2V617F* allele burden is shown in Figure 4 for the region where E_C is stable. Perturbation of a parameter may improve or impair prognosis when the coexistence point is the stable attractor. The top panel of Figure 4, shows that decreasing C and \mathcal{R} improve prognosis by lowering the allele burden. Contrarily, increasing I , causes a decay in allele burden. This suggests that inflammatory inhibitors could counteract treatments in this case. In other cases, increasing I typically leads to a worse prognosis, considering Figure 2.

The model presented here may inform clinical practice to make group specific treatment protocols with particular focus on the inflammatory components which may accelerate or dampen the disease progression. Interventions should address decreasing C and \mathcal{R} and potentially I but the latter depends on the remaining parameter values as adverse effects may be observed.

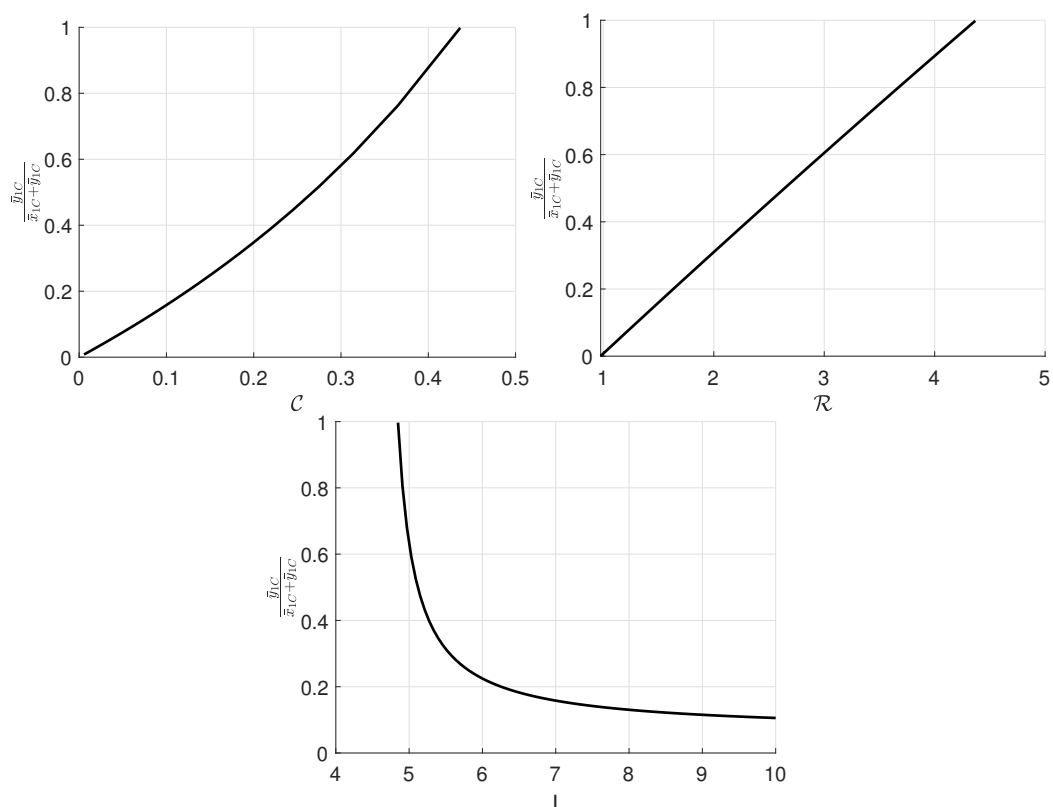


Figure 4. Allele burden (the ratio of \bar{y}_{1c} to the total number of \bar{x}_{1c} and \bar{y}_{1c}) at the steady state for the region where the co-existing steady state is stable. On the top, left and right panels show that by increasing C and \mathcal{R} , allele burden also increases. On the contrary, increasing I reduces the allele burden. In the top panel $\mathcal{R} = 1.5$ and $I = 7$, in the top right, $C = 0.1$ and $I = 7$ and in the bottom panel, $\mathcal{R} = 1.5$ and $C = 0.1$.

Conflict of interest

No conflict of interest.

References

1. P. J. Campbell and A. R. Green, The myeloproliferative disorders, *N. Engl. J. Med.*, **355** (2006), 2452–2466.
2. H. C. Hasselbalch, Chronic inflammation as a promotor of mutagenesis in essential thrombocythemia , polycythemia vera and myelofibrosis. A human inflammation model for cancer development?, *Leukemia Res.*, **37** (2013), 214–220.
3. H. C. Hasselbalch, Perspectives on chronic inflammation in essential thrombocythemia , polycythemia vera , and myelofibrosis: is chronic inflammation a trigger and driver of clonal evolution and development of accelerated atherosclerosis and second cancer?, *Blood*, **119** (2012), 3219–3226.
4. S. Y. Kristinsson, O. Landgren, J. Samuelsson, et al., Autoimmunity and the risk of myeloproliferative neoplasms, *Haematologica*, **95** (2010), 1216–1220.
5. M. Andersen, Z. Sajid, R. K. Pedersen, et al., Mathematical modelling as a proof of concept for MPNs as a human inflammation model for cancer development, *Plos One*, **12** (2017), 1–18.
6. T. Barbui, A. Carobbio, G. Finazzi, et al., Inflammation and thrombosis in essential thrombocythemia and polycythemia vera : different role of C-reactive protein and pentraxin 3, *Haematologica*, **96** (2011), 315–318.
7. N. L. Komarova, Principles of regulation of self-renewing cell lineages, *Plos One*, **8** (2013).
8. N. L. Komarova and P. van den Driessche, Stability of control networks in autonomous homeostatic regulation of stem cell lineages, *B. Math. Biol.*, **80** (2015), 1345–1365.
9. J. Yang, D. E. Axelrod and N. L. Komarova, Determining the control networks regulating stem cell lineages in colonic crypts, *J. Theor. Biol.*, **429** (2017), 190–203 .
10. F. Michor, Y. Iwasa and M. A. Nowak, Dynamics of cancer progression, *Nature Rev. Cancer*, **4** (2004), 197–205.
11. F. Michor, T. P. Hughes, Y. Iwasa, et al., Dynamics of chronic myeloid leukaemia, *Nature*, **435** (2005), 1267–1270.
12. D. Dingli and F. Michor, Successful Therapy Must Eradicate Cancer Stem Cells, *Stem Cells*, **24** (2006), 2603–2610.
13. G. Clapp, T. Lepoutre, R. El Cheikh, et al., Implication of autologous immune system in bcr-abl transcript variations in chronic myelogenous leukemia patients treated with imatinib, *Cancer Res.*, **75** (2015), 4053–4062.
14. T. Stiehl and A. Marciniak-Czochra, Mathematical modelling of leukemogenesis and cancer stem cell dynamics, *Math. Model. Nat. Phenom.*, **7** (2012), 166–202.
15. T. Stiehl, A. D. Ho and A. Marciniak-Czochra, Mathematical modelling of the impact of cytokine response of acute myeloid leukemia cells on patient prognosis, *Sci. Rep.*, **2809** (2018).

16. H. Haeno, R. L. Levine, D. G. Gilliland, et al., A progenitor cell origin of myeloid malignancies, *Proc. Natl. Acad. Sci. USA*, **106** (2009), 16616–16621.
17. J. Zhang, A. G. Fleischman, D. Wodarz, et al., Determining the role of inflammation in the selection of JAK2 mutant cells in myeloproliferative neoplasms, *J. Theor. Biol.*, **425** (2017), 43–52.
18. J. T. Ottesen, Z. Sajid, R. K. Pedersen, et al., Bridging blood cancers and inflammation: The reduced Cancitis model, *J. Theor. Biol.*, **465** (2019), 90–108.
19. C. Walkley, J. Shea, N. Sims, et al., Rb regulates interactions between hematopoietic stem cells and their bone marrow microenvironment, *Cell*, **129** (2007), 1081–1095.
20. T. Stiehl, N. Baran, A. D. Ho, et al., Cell division patterns in acute myeloid leukemia stem-like cells determine clinical course: A model to predict patient survival, *Cancer Res.*, **75** (2015), 940–949.
21. T. Walenda, T. Stiehl, H. Braun, et al., Feedback Signals in Myelodysplastic Syndromes: Increased Self-Renewal of the Malignant Clone Suppresses Normal Hematopoiesis, *PLoS Comput. Biol.*, **10** (2014), e1003599.
22. Y. W. Kim, B. K. Koo, H. W. Jeong, et al., Defective Notch activation in microenvironment leads to myeloproliferative disease, *Blood*, **112** (2008), 4628–4638.
23. K. Y. King and M. A. Goodell, Inflammatory modulation of hematopoietic stem cells: viewing the hematopoietic stem cell as a foundation for the immune response, *Nat. Rev. Immunol.*, **11** (2014), 685–692.
24. E. Rovida, I. Marzi, M. G. Cipolleschi, et al., One more stem cell niche: how the sensitivity of chronic myeloid leukemia cells to imatinib mesylate is modulated within a “hypoxic” environment, *Hypoxia*, (2014), 1–10.
25. A. Marciniak-Czochra, T. Stiehl, A. D. Ho, et al., Modeling of asymmetric cell division in hematopoietic stem cells—regulation of self-renewal is essential for efficient repopulation, *Stem Cells Dev.*, **18** (2009), 377–385.
26. A. L. Jackson and L. A. Loeb, The mutation rate and cancer, *Eur. J. Haematol.*, **97** (2016), 63–69.
27. A. Knutson, Mutation and Cancer: Statistical study of retinoblastoma, *Proc. Natl. Acad. Sci. USA*, **68** (1971), 820–823.
28. F. Michor, Y. Iwasa and N. MA, The age incidence of chronic myeloid leukemia can be explained by a one-mutation model, *Proc. Natl. Acad. Sci. USA*, **103** (2006), 14931–14934.
29. F. Michor, Mathematical models of cancer stem cells, *J. Clin. Oncol.*, **26** (2008), 2854–2861.
30. E. Voit, A first course in system biology, *Garland Science, Taylor & Francis Group, New York and London*, **68** (2013).
31. A. L. Sørensen and H. C. Hasselbalch, Smoking and Philadelphia-negative chronic myeloproliferative neoplasms, *Genetics*, **148** (1998), 1483–1490.
32. H. C. Hasselbalch, Smoking as a contributing factor for development of polycythemia vera and related neoplasms, *Leukemia Res.*, **015** (2015).
33. V. A. Kuznetsov and G. D. Knott, Modeling tumor regrowth and immunotherapy, *Math. Comput. Model.*, **33** (2001), 1275–1287.

34. C. Robinson, Dynamical Systems, Stability, Symbolic Dynamics, and Chaos, in *Second CRC Press, Boca Raton, Fla., 1999.*

Supplementary

Stability analysis of Steady states:

At $E_{H\pm}$ the Jacobian of the **purely hematopoietic steady state** becomes,

$$J_{E_H} = \begin{bmatrix} a_{11} & 0 & a_{13} & 0 & 0 & a_{16} \\ a_{21} & a_{22} & 0 & 0 & 0 & 0 \\ 0 & 0 & a_{33} & 0 & 0 & 0 \\ 0 & 0 & a_{43} & a_{44} & 0 & 0 \\ a_{51} & a_{52} & a_{53} & a_{54} & a_{55} & a_{56} \\ 0 & 0 & 0 & 0 & a_{65} & a_{66} \end{bmatrix} \quad (\text{S.1})$$

where

$$a_{11} = r_x \left(\frac{\bar{s}_H}{(1+c_{xx}\bar{x}_{0H})^2} - \alpha_x \right),$$

$$a_{13} = -\frac{r_x c_{xy} \bar{s}_H \bar{x}_{0H}}{(1+c_{xx}\bar{x}_{0H})^2},$$

$$a_{16} = \frac{r_x \bar{x}_{0H}}{(1+c_{xx}\bar{x}_{0H})},$$

$$a_{21} = a_x A_x,$$

$$a_{22} = -d_{x1},$$

$$a_{33} = r_y \left(\frac{\bar{s}_H}{1+c_{yx}\bar{x}_{0H}} - \alpha_y \right),$$

$$a_{43} = a_y A_y,$$

$$a_{44} = -d_{y1},$$

$$a_{51} = d_{x0},$$

$$a_{52} = d_{x1},$$

$$a_{53} = d_{y0},$$

$$a_{54} = d_{y1},$$

$$a_{55} = -e_a \bar{s}_H,$$

$$a_{56} = -e_a \bar{a}_H,$$

$$a_{65} = r_s,$$

$$a_{66} = -e_s,$$

and rest of the elements of J_{E_H} are zero.

At $E_{L\pm}$ the Jacobian of the **purely malignant steady state**.

$$J_{E_L} = \begin{bmatrix} a_{11} & 0 & 0 & 0 & 0 & 0 \\ a_{21} & a_{22} & 0 & 0 & 0 & 0 \\ a_{31} & 0 & a_{33} & 0 & 0 & a_{36} \\ 0 & 0 & a_{43} & a_{44} & 0 & 0 \\ a_{51} & a_{52} & a_{53} & a_{54} & a_{55} & a_{56} \\ 0 & 0 & 0 & 0 & a_{65} & a_{66} \end{bmatrix} \quad (\text{S.2})$$

where

$$\begin{aligned}
 a_{11} &= r_x \left(\frac{\bar{s}_L}{1+c_{xy}\bar{y}_{0L}} - \alpha_x \right), \\
 a_{21} &= a_x A_x, \\
 a_{22} &= -d_{x1}, \\
 a_{31} &= -\frac{r_y c_{yx} \bar{s}_L \bar{y}_{0L}}{(1+c_{yy}\bar{y}_{0L})^2}, \\
 a_{33} &= r_y \left(\frac{\bar{s}_L}{(1+c_{yy}\bar{y}_{0L})^2} - \alpha_y \right), \\
 a_{36} &= \frac{r_y \bar{y}_{0L}}{1+c_{yy}\bar{y}_{0L}}, \\
 a_{43} &= a_y A_y, \\
 a_{44} &= -d_{y1}, \\
 a_{51} &= d_{x0}, \\
 a_{52} &= d_{x1}, \\
 a_{53} &= d_{y0}, \\
 a_{54} &= d_{y1}, \\
 a_{55} &= -e_a \bar{s}_L, \\
 a_{56} &= -e_a \bar{a}_L, \\
 a_{65} &= r_s, \\
 a_{66} &= -e_s
 \end{aligned}$$

and rest of the elements of array are zero.

At $E_{C\pm}$ the Jacobian of the **co-existing steady state** becomes,

$$J_{EC} = \begin{bmatrix} a_{11} & 0 & a_{13} & 0 & 0 & a_{16} \\ a_{21} & a_{22} & 0 & 0 & 0 & 0 \\ a_{31} & 0 & a_{33} & 0 & 0 & a_{36} \\ 0 & 0 & a_{43} & a_{44} & 0 & 0 \\ a_{51} & a_{52} & a_{53} & a_{54} & a_{55} & a_{56} \\ 0 & 0 & 0 & 0 & a_{65} & a_{66} \end{bmatrix} \quad (\text{S.3})$$

where

$$\begin{aligned}
 a_{11} &= r_x \left(\frac{\bar{s}_C}{(1+c_{xx}\bar{x}_{0C}+c_{xy}\bar{y}_{0C})^2} - \alpha_x \right), \\
 a_{13} &= -\frac{r_x c_{xy} \bar{s}_C \bar{x}_{0C}}{(1+c_{xx}\bar{x}_{0C}+c_{xy}\bar{y}_{0C})^2}, \\
 a_{16} &= \frac{r_x \bar{x}_{0C}}{(1+c_{xx}\bar{x}_{0C}+c_{xy}\bar{y}_{0C})}, \\
 a_{21} &= a_x A_x, \\
 a_{22} &= -d_{x1}, \\
 a_{31} &= -\frac{r_y c_{yx} \bar{s}_C \bar{y}_{0C}}{(1+c_{yx}\bar{x}_{0C}+c_{yy}\bar{y}_{0C})^2}, \\
 a_{33} &= r_y \left(\frac{\bar{s}_C}{(1+c_{yx}\bar{x}_{0C}+c_{yy}\bar{y}_{0C})^2} - \alpha_y \right), \\
 a_{36} &= \frac{r_y \bar{y}_{0C}}{(1+c_{yx}\bar{x}_{0C}+c_{yy}\bar{y}_{0C})}, \\
 a_{43} &= a_y A_y, \\
 a_{44} &= -d_{y1}, \\
 a_{51} &= d_{x0}, \\
 a_{52} &= d_{x1}, \\
 a_{53} &= d_{y0},
 \end{aligned}$$

$$a_{54} = d_{y1},$$

$$a_{55} = -e_a \bar{s}_C,$$

$$a_{56} = -e_a \bar{a}_C,$$

$$a_{65} = r_s,$$

$$a_{66} = -e_s$$

and rest of the elements of the J_{E_C} are zero.



AIMS Press

©2019 the Author(s), licensee AIMS Press. This is an open access article distributed under the terms of the Creative Commons Attribution License (<http://creativecommons.org/licenses/by/4.0>)